

See discussions, stats, and author profiles for this publication at: <https://www.researchgate.net/publication/257975001>

Ligand exchange leads to efficient triplet energy transfer to CdSe/ZnS Q-dots in a poly(N-vinylcarbazole) matrix nanocomposite

ARTICLE in JOURNAL OF APPLIED PHYSICS · FEBRUARY 2013

Impact Factor: 2.18 · DOI: 10.1063/1.4793266

CITATIONS

8

READS

54

11 AUTHORS, INCLUDING:



Eduard Fron

University of Leuven

63 PUBLICATIONS 796 CITATIONS

SEE PROFILE



Wim Dehaen

University of Leuven

568 PUBLICATIONS 9,277 CITATIONS

SEE PROFILE



Hens Zeger

Ghent University

179 PUBLICATIONS 3,369 CITATIONS

SEE PROFILE



Mark Van der Auweraer

University of Leuven

333 PUBLICATIONS 8,467 CITATIONS

SEE PROFILE

Ligand exchange leads to efficient triplet energy transfer to CdSe/ZnS Q-dots in a poly(N-vinylcarbazole) matrix nanocomposite

Adis Khetubol, Sven Van Snick, Antti Hassinen, Eduard Fron, Yuliar Firdaus, Lesley Pandey, Charlotte C. David, Karel Duerinckx, Wim Dehaen, Zeger Hens, and Mark Van der Auweraer

Citation: *Journal of Applied Physics* **113**, 083507 (2013); doi: 10.1063/1.4793266

View online: <http://dx.doi.org/10.1063/1.4793266>

View Table of Contents: <http://scitation.aip.org/content/aip/journal/jap/113/8?ver=pdfcov>

Published by the AIP Publishing

Articles you may be interested in

Photo-instability of CdSe/ZnS quantum dots in poly(methylmethacrylate) film

J. Appl. Phys. **114**, 244308 (2013); 10.1063/1.4857055

Study of hole mobility in poly(N-vinylcarbazole) films doped with CdSe/ZnS quantum dots encapsulated by 11-(N-carbazolyl) undecanoic acid (C11)

J. Appl. Phys. **114**, 173704 (2013); 10.1063/1.4827395

Aqueous based synthesis of CdSe/ZnS Q-dots: Study on luminescence properties and cytotoxicity

AIP Conf. Proc. **1536**, 63 (2013); 10.1063/1.4810101

Electrical control of photoluminescence wavelength from semiconductor quantum dots in a ferroelectric polymer matrix

Appl. Phys. Lett. **99**, 153112 (2011); 10.1063/1.3651322

Dispersion of Cd X (X = Se , Te) nanoparticles in P3HT conjugated polymer

J. Renewable Sustainable Energy **1**, 023107 (2009); 10.1063/1.3101815

The advertisement features a blue background with a stylized orange and yellow film strip on the left. The text is in white and orange. The main headline reads 'Not all AFMs are created equal' in orange, followed by 'Asylum Research Cypher™ AFMs' in white, and 'There's no other AFM like Cypher' in orange. Below this is the website 'www.AsylumResearch.com/NoOtherAFMLikeIt' in white. In the bottom right corner is the Oxford Instruments logo, which consists of the word 'OXFORD' above 'INSTRUMENTS' inside a square frame, with the tagline 'The Business of Science®' below it.

Ligand exchange leads to efficient triplet energy transfer to CdSe/ZnS Q-dots in a poly(*N*-vinylcarbazole) matrix nanocomposite

Adis Khetubol,¹ Sven Van Snick,² Antti Hassinen,³ Eduard Fron,¹ Yuliar Firdaus,¹ Lesley Pandey,¹ Charlotte C. David,¹ Karel Duerinckx,¹ Wim Dehaen,² Zeger Hens,³ and Mark Van der Auweraer^{1,a)}

¹Laboratory of Photochemistry and Spectroscopy, Division of Molecular Imaging and Photonics, Chemistry Department, KULeuven, Celestijnenlaan 200F, B2404, 3001 Leuven, Belgium

²Laboratory of Organic Synthesis, Division of Molecular Design and Synthesis, Chemistry Department, KULeuven, Celestijnenlaan 200F, B2404, 3001 Leuven, Belgium

³Physics and Chemistry of Nanostructures, Ghent University, Krijgslaan 281-S3, 9000 Gent, Belgium

(Received 27 September 2012; accepted 6 February 2013; published online 25 February 2013)

Upon exchanging long chain alkylamine ligands with a carbazole terminated fatty acid as 6-(*N*-carbazolyl)-hexanoic acid (C6) and 11-(*N*-carbazolyl) undecanoic acid (C11), efficient photoluminescence (PL) of CdSe/ZnS colloidal quantum dots (QDs) was observed upon excitation in the absorption band of the carbazole moiety at 330 nm. This effect, which occurred both in solution and in a poly(*N*-vinylcarbazole) (PVK) matrix doped with the QDs, is attributed to sensitization of the QDs by PVK and the ligands. More efficient energy transfer was observed in solution for the shorter ligand (C6) capped QDs, due to a shorter average distance between the donor (carbazole) and the acceptor (QD). The binding of C6 and C11 to the QDs was confirmed by ¹H solution nuclear magnetic resonance, which showed line broadening of the carbazole signal due to a decrease of the mobility of the carbazoles upon binding to the QDs compared with the sharp lines observed for the free molecules in solution. In doped PVK films, the significant enhancement of the energy transfer to the QD core could also be related to a better miscibility between the QDs and the PVK as confirmed by optical transmission and confocal microscopy images. In contrast to the experiment in solution, the overall energy transfer in the doped films was found more efficient for QDs capped with C11. To study in more detail the energy transfer between the carbazole moieties and the QDs, time-resolved fluorescence measurements were performed for solutions of C6 and C11, capped QDs and PVK films doped with the QDs. In contrast to the large enhancement of the QD emission indicated by steady-state PL spectra, the latter experiments suggested only a relatively low efficiency (19.6% and 10.8%) for singlet transfer from the carbazole ligands to the QDs. This suggests that the enhancement of the QD emission must be largely due to triplet transfer. © 2013 American Institute of Physics. [<http://dx.doi.org/10.1063/1.4793266>]

I. INTRODUCTION

Organic light emitting diodes (OLEDs) and polymer OLEDs (PLEDs) have become attractive due to their potential applications particularly in display and lighting applications. The unique advantages of OLED and PLED displays, such as low power consumption, wide viewing angle, high contrast, etc., have driven efforts of enhancing their efficiency, life time, and color stability.^{1–3}

Due to spin statistics, 75% of electron-hole recombination in OLEDs leads to a non-luminescent triplet state, which limits the efficiency of the devices. Therefore, the matrix of the OLED or PLED is doped by a guest that is able to emit from the triplet state. In these doped systems, triplet excitation transfer from the matrix to the guest is followed by emission from the triplet state of the guest. Over a decade, several groups developed organo-transition metal compounds as triplet emitting guest materials for low molecular weight matrices^{4–10} and conjugated polymer matrices.^{11–13}

While for the combination of low molecular weight matrices and green or red emitting guests excellent results were obtained, it proved to be more difficult to find a good combination of a matrix and a guest yielding blue emission.^{10,14,15}

For conjugated polymer matrices, which are processed from solution, colloidal semiconductor nanocrystals are in principle a good alternative to such transition metal complexes considering their high luminescent quantum yield (QY) (>40% for core/shell particles) (photo)chemical stability, emission tunability over the visible wavelength range, narrow emission spectra (full width at half height, FWHM < 40 nm), and close proximity of singlet and triplet levels. They offer furthermore the advantage of a much shorter decay time of the emitting excited state, decreasing in this way the occurrence of different exciton annihilation processes.

In purely inorganic devices semiconductor nanocrystal-based II–VI compounds, such as CdSe, CdS, CdTe, etc., have particularly played a role in a new generation of optoelectronic applications.^{16–19} The development of state of the art synthesis leads to further improvement of the chemical stability and fluorescence QY of the nanocrystals through surface passivation, and/or the synthesis of quantum dots

^{a)}Author to whom correspondence should be addressed. Electronic mail: mark.vanderauweraer@chem.kuleuven.be.

(QDs) with a core/shell nanostructure.^{20–23} However, the possibility to use such QDs to harvest the non-emitting triplets of the matrix requires that efficient triplet transfer to the QDs occurs and that the initially populated triplet excited state of the QDs is efficiently converted into an emitting singlet state. The latter can be expected due to the very small singlet–triplet gap in the QDs.²⁴

We focused on the use of CdSe/ZnS core/shell QDs because the wavelength requirements for absorption and emission allowed the use of relatively small (2.2 nm) QDs. In this way, a large concentration and efficient energy transfer could be obtained while minimizing the loading (in wt. % or vol. %) of the polymer by the QDs. Although the use of these QDs has already been investigated in combination with conductive polymers in hybrid LEDs^{22,25–36} the results were quite disappointing. A plausible explanation for these poor results could be the limited miscibility of the QDs with the matrix leading to clustering and deterioration of the film morphology. This prompted us to develop and extensively study a novel light emitting material based on an electroluminescent polymer doped with blue-emitting CdSe/ZnS QDs. Rizzo *et al.* constructed an OLED with an emitting layer consisting of a low molecular weight emitter and CdSe QDs.³⁷ In this way, they developed an alternative to reduce the problems associated with the miscibility of the polymer and the QDs. Another alternative to avoid the problems associated with the mixing is the deposition of a (single) emitting layer of QDs between two polymers of low molecular weight layers of an organic compound.^{20,36,38,39}

Although better performing blue emitting conjugated polymers exist for the moment, we chose to use poly(*N*-vinylcarbazole) (PVK) for the proof of principle experiments because of the large amount of experimental information available on this polymer and its commercial availability. In spite of some shortcomings, PVK can be considered as a benchmark material for OLED applications, especially when blue emission is required. Over decades, its optical, photophysical, photochemical, and charge transport properties as well as its applications as a light source, a host material and/or a hole transport material in PLEDs have been studied.^{40–49} Due to their specific properties such as (photo)chemical stability and high triplet energy, PVK and related carbazole polymers become an excellent choice as host materials for blue emitting triplet emitters and semiconductor QDs.^{44,50–53} From an experimental point of view PVK is also a good choice as it is characterized by, in contrast to many conjugated polymers, an appreciable intersystem crossing (ISC) and low singlet exciton mobility. The

latter aspects are important in minimizing the sensitization of the QDs by singlet transfer and in maximizing the sensitization of the QDs by triplet transfer, which is advantageous for the study of triplet energy transfer to the QDs.

To optimize their photophysical properties, to minimize the trapping of electrons and holes at the defect sites and to avoid aggregation, QDs are generally coated by an organic ligand. It is clear that when the QDs are incorporated in a polymer this ligand will be a barrier for the transfer of energy and carriers. Generally organic molecules such as trioctylphosphine oxide (TOPO), oleic acid, oleylamine, alkylamines, etc. are used for encapsulating nanocrystals during and after synthesis. Most of these commonly used ligands are insulating, due to a wide optical bandgap ($\sigma - \sigma^*$ or wide $\pi - \pi^*$), which could hinder the expected transfer of charges and/or excitons between the polymer and the QDs. Furthermore, the ligand coating must be sufficiently miscible with the polymer to avoid phase separation at the relatively high loading necessary for efficient energy and/or charge carrier transfer.^{32–34} In this paper, we report on the enhancement of the miscibility and therefore of the efficiency for triplet energy transfer towards CdSe/ZnS QDs using fatty acid ligands terminated by a carbazole group (6-(*N*-carbazolyl) hexanoic acid (C6) and 11-(*N*-carbazolyl) undecanoic acid (C11)) (Chart 1).

II. EXPERIMENTAL

A. Materials

PVK with $M_w \approx 1\,100\,000$ was purchased from Sigma-Aldrich. Long-chain alkylamine (LCA) capped QDs with the first exciton absorption peak of 460 nm were purchased from Evident technology. The QDs give blue emission with the emission maxima of 480 nm upon excitation of the semiconductor between 300 and 460 nm. The approximate core's diameter of 2.05 nm was obtained according to the fitting function for the spectra of CdSe QDs reported by Yu *et al.*⁵⁴ As described below the existing ligand was replaced by a carbazole terminated fatty acid. The carbazole ligands, C6 and C11 with different alkyl-chain lengths, were synthesized according to the procedure in Subsection II B. The molecular structures of PVK, LCA, C6, and C11 are presented in Chart 1.

All necessary solvents used in this work, acetone, acetonitrile (ACN), chlorobenzene (CB), 2-methyltetrahydrofuran (methyl-THF), methanol, and chloroform-*d*, are spectroscopic grade. They were purchased from Acros and Sigma-Aldrich and used as received.

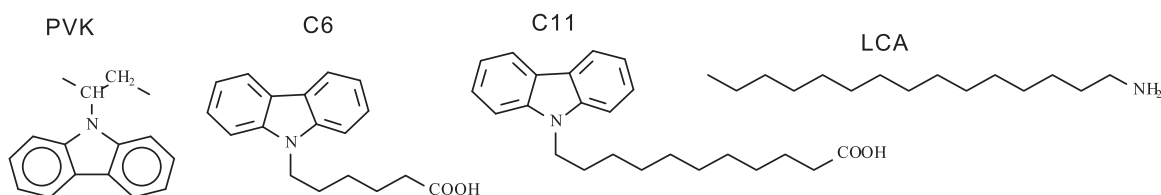


CHART 1. Molecular structures of PVK, C6, C11, and LCA.

B. Synthesis and characterization of C6 and C11

General procedure 1. Synthesis of bromo esters: To a well-stirred solution of the appropriate bromo acid (5000 mg) in methanol (100 ml) was added a catalytic amount of concentrated sulphuric acid. The reaction mixture was heated to reflux and stirred overnight. To the mixture was then added a saturated solution of NaHCO_3 until no more CO_2 evolved, followed by extraction with diethylether (3×50 ml). The organic layers were combined, washed with brine, dried on anhydrous MgSO_4 , and concentrated by rotary evaporation. For details, see Supplementary material.⁵⁵

General procedure 2. Synthesis of carbazole ligands: To a suspension of K_2CO_3 in CH_3CN were added carbazole and the appropriate bromo ester in one portion. The reaction mixture was heated to reflux and stirred for 3 days. The inorganic salts were removed by filtration and the filtrate was concentrated by rotary evaporation. Purification by column chromatography (petroleum ether ethylacetate 8/2) yielded a yellow oil, to which 10 ml NaOH (2M) was added. Stirring overnight at 100°C resulted in a transparent solution from which the carbazole ligand was precipitated by acidifying the reaction mixture. The precipitate was filtered, washed with H_2O (3×10 ml), and dried *in vacuo*. For details, see Supplementary material.

C. Ligand exchange

The commercial LCA capped QDs were originally provided in toluene (TL) at a concentration of 40 mg/ml. (This value is referred to the total weight of QDs, e.g., core, shell, and LCA ligands.) Since C6 and C11 cannot be dissolved in TL, we selected CB as solvent for the ligand exchange.

First, the solvent of the QDs (TL) was replaced by CB. Therefore, QDs were precipitated by addition of ACN to the TL solution, followed by centrifugation. Then, the precipitate was redispersed by addition of CB at three times the initial volume of the TL solution with LCA capped QDs to which an amount of C6 (or C11) corresponding to about 100 molecules of ligand per QD was added. In this way, a solution of 13 mg/ml of LCA capped QDs was obtained. The ligand exchange was performed by stirring the solution of the LCA coated QDs and the new ligands for 30 min at 60°C . Then, the QDs were precipitated from the solution by adding slowly a 1:1 mixture (by volume) of ACN and methanol until the transparent solution became slightly turbid. After centrifugation and removing the liquid (containing excess C6 or C11 and dissociated LCA ligands), the QDs were redissolved in CB. The ligand exchange was repeated one more time following the previous procedure. Purification was performed after the ligand exchange at least two times by following the precipitation procedure described earlier to make sure that the residual excess ligands were completely removed. After the ligand exchange and purification, the QDs were finally dissolved again in CB. The concentration of the QDs after the ligand exchange was calculated by comparing the optical density at the first excitation peak of a diluted QD solution with that of the solution obtained from EVIDOT (QDs with LCA). The molarity of the eventual

solution of carbazole terminated quantum dots could then be estimated by comparing the absorbance of the solution to that of the solution provided by EVIDOT, taking into account that the product's data sheet (EVIDOT) indicates a molecular weight of $\sim 92.3 \mu\text{g/nmol}$ for the LCA capped QDs (core + shell + ligands).

D. Sample preparation

For all the solution samples used for photoluminescence (PL) measurements, quantum yield determination, and time-resolved PL measurement, the solution was diluted until the optical density was approximately 0.1 at the excitation wavelength. Pristine C6 and C11 solutions for nuclear magnetic resonance (NMR) measurements were prepared in CDCl_3 at an approximate concentration of 10 mg/ml. C6 and C11 capped QDs for NMR measurements were prepared by the ligand exchange procedure given in Sec. II C. However, after the second ligand exchange (in CB) the QDs were dissolved and purified in deuterated chloroform (CDCl_3). After determining their concentration, the QD samples for ligand quantification were further diluted until a concentration corresponding to 15 mg/ml (estimated to be 1.6×10^{-4} M using the procedure discussed in Sec. II C) was achieved. The ligand grafting density was quantified by adding a known amount of CH_2Br_2 ($2.5 \mu\text{l}$ or 3.56×10^{-5} mol at 25°C) to 800 μl of the QD solutions for the final molecular ratio of 1:274 of QD: CH_2Br_2 .

Glass substrates for thin film samples were cleaned by acetone, an alkaline surfactant solution for cleaning and water and subsequently dried with N_2 . PVK and doped PVK (with QDs) solutions were prepared based on a fixed concentration of PVK (20 mg/ml). The spin-coating speed of 1000 rpm was applied for all the films.

E. Sample characterization

^1H and ^{13}C NMR spectra were recorded on a Bruker Avance 300 (300 MHz, ^1H ; 75 MHz, ^{13}C) instrument. The chemical shifts are reported in parts per million relative to tetramethylsilane using the residual solvent signal as internal reference. Multiplicities are indicated by s (singlet), d (doublet), t (triplet), q (quartet), qu (quintet), m (multiplet), and bs (broad singlet). Coupling constants, J, are reported in Hertz. Mass spectra were recorded by using a Kratos MS50TC and a Kratos Mach III data system. The ion source temperature was 150 – 250°C as required. High resolution EI-mass spectra were performed with a resolution of 10 000. The low resolution spectra were obtained with a HP5989A MS instrument. For column chromatography, silica supplied by Acros Organics (0.060–0.200 mm 60 Å) was used. Visualization was accomplished with TLC-plates supplied by MERCK (TLC Silica gel 60 F₂₅₄ (254 nm)).

Steady state absorption and corrected PL spectra were recorded with a Lambda 40 (Perkin-Elmer) and SPEX Fluorolog spectrophotometer, respectively. The fluorometer allowed us to correct for the wavelength dependence of the sensitivity of the detection system. Fluorescence QYs of the solution samples of carbazole ligands in CB and of the PVK film at the excitation of 330 nm were obtained using a

solution of quinine sulfate in 0.1N H₂SO₄ as a reference standard.

The fluorescence decays were determined by the single photon timing method. The excitation wavelengths of 330 nm and 460 nm were obtained using, respectively, the third and second harmonic of a Ti:sapphire laser (Tsunami, Spectra Physics) with a repetition rate of 8.1 MHz using a pulse picker (GWU). The detection system consists of a subtractive double monochromator (9030DS, Scientech) and a micro-channel plate photomultiplier (R3809U, Hamamatsu). Fluorescence decays were recorded under magic angle polarization. A time-to-amplitude converter (TAC), and an analog-to-digital converter (ADC) on a PC board (PICOQUANT) were used to obtain the fluorescence decay histograms in 4096 channels with time increments of 20–30 ps in this case. The time decays were globally analyzed with a time-resolved fluorescence analysis (TRFA) software based on a standard criterion value, $\chi^2 < 1.1$.⁵⁶

Confocal fluorescence images were acquired with a laser scanning microscope (Fluoview FV1000; Olympus, Tokyo, Japan) equipped with a 440 nm diode laser (Spectra Physics, Irvine, CA, USA). The objective and the excitation dichroic mirror used were UPlan SApo100 \times /1.40 and DM458/515, respectively (Olympus). The image size was adjusted to 512 \times 512 pixels, with the pixel size corresponding to \sim 50 nm. The pixel dwelling time was 4 μ s/pixel, and a 4 \times Kalman filter was applied to reduce noise in the image. Fluorescence signals were recorded from 470 to 570 nm. The transmission micrographs were monitored visually via an optical microscope OPTIPHOT-2 (Nikon OPTIPHOT-2) and the micrographs were recorded using a digital camera (Nikon 995).

III. RESULTS AND DISCUSSION

A. NMR experiments

¹H NMR was used to confirm the binding of the C6 and C11 ligands to dissolved QDs. Fig. 1 shows the aromatic part of the ¹H NMR spectra of the free ligand and a solution of the QDs after ligand exchange in a CDCl₃ solution for C6

(a) and C11 (b). Upon binding to the QDs the T₂ of the carbazole protons decreases drastically due to decreased mobility leading to broad lines. Those lines are situated at the same chemical shift as those of the different aromatic protons of a solution of C6 and C11 in CDCl₃. The absence of narrow signals of the carbazole protons in the solution of the C6 and C11 capped QDs indicates that after the purification procedure used no more free ligands are present. The sharp peak at \sim 7.26 ppm, which is clearly seen in both spectra of the QD solutions, is attributed to the NMR signal of residual CHCl₃ in the solvent (CDCl₃).⁵⁷ Due to the much higher peak intensities of the carbazole signals in a solution of the free ligands, this signal cannot be detected in the solutions of C6 and C11 in CDCl₃.

By adding a known amount of CH₂Br₂ (see Sec. II D) to the solution with a known amount of the C6 and C11 capped QDs, the number of ligands per QD can be estimated. ¹H NMR spectra of the free ligand and the QDs after the ligand exchange (to the latter solution CH₂Br₂ was added) are shown in Fig. 2(a) for C6 and Fig. 2(b) for C11. The sharp peak at \sim 4.8 ppm in the solutions containing the ligand exchanged QDs is attributed to CH₂Br₂. From the ratio of the area under the CH₂Br₂ resonance and the area under one of the carbazole resonances which was normalized to one, a number of 76 and 44 ligands/QD were estimated for, respectively, C6 and C11. Similar results were obtained when the area of the signal of the CH₂—N protons at 4.2 ppm was compared to that of the protons of CH₂Br₂. More details on the use of NMR for identification and quantification of organic ligands of colloidal nanocrystals have been reported by Moreels *et al.*⁵⁸

B. Stationary absorption and emission spectra

Optical absorption and PL spectra of PVK (film) and colloidal QDs with LCA capping (CB solution) are shown in Fig. 3(a). The PL spectra of the PVK and QD samples were obtained at an excitation wavelength (λ_{exc}) of 330 nm and 400 nm, respectively. The large overlap between PVK emission and QD absorption spectra suggests the possibility of

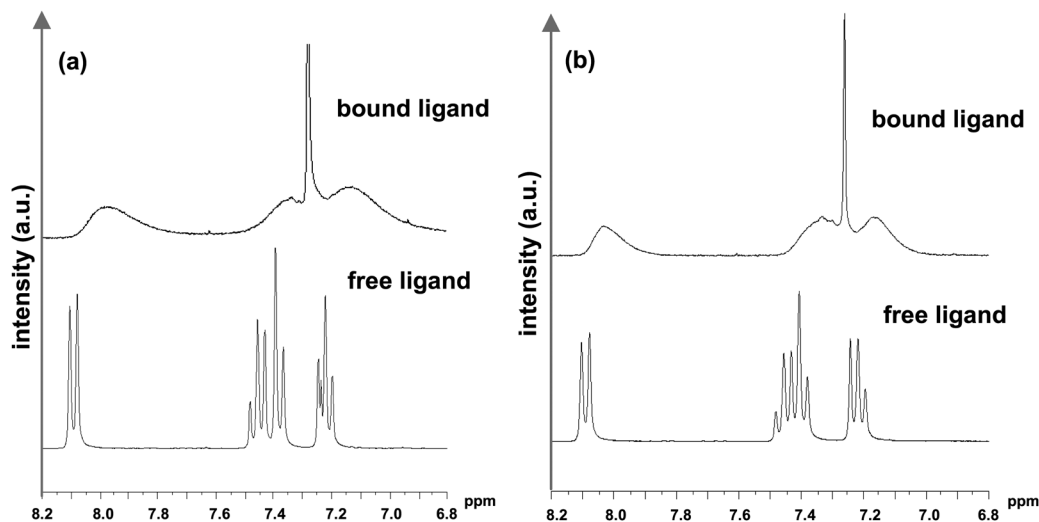


FIG. 1. ¹H spectra of the aromatic part of the pristine carbazole ligands and the QDs after the ligand exchange for C6 (a) and C11 (b) in CDCl₃.

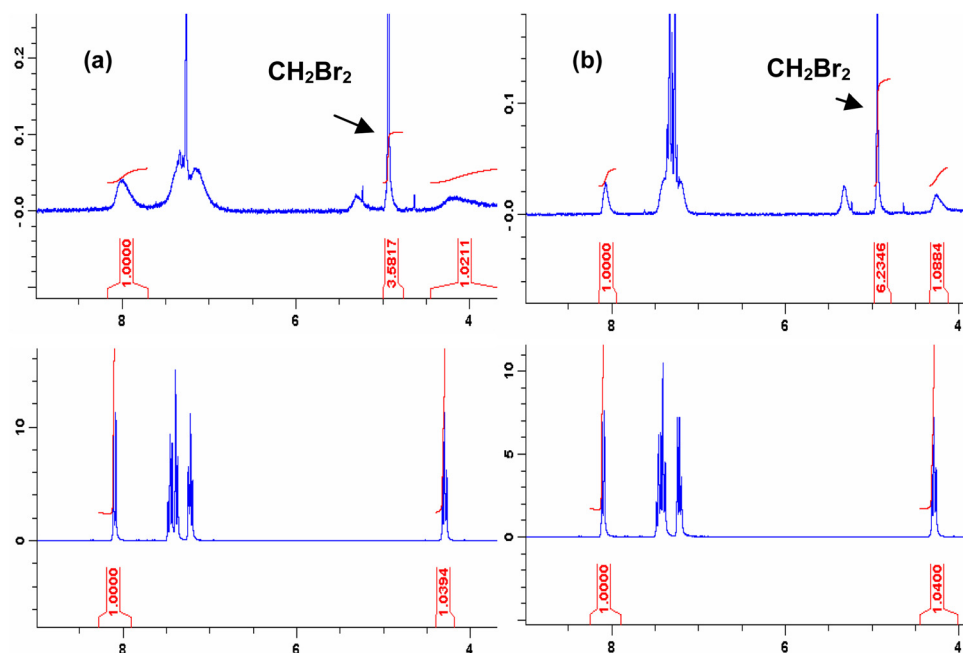


FIG. 2. ^1H spectra of pristine carbazole ligands (lower part) and QDs (upper part) in CDCl_3 after the ligand exchange with the addition of CH_2Br_2 for C6 (a) and C11 (b).

singlet energy transfer from PVK to QDs using either Förster or Dexter transfer.⁵⁹ Fig. 3(b) shows the absorption and PL spectra ($\lambda_{\text{exc}} = 330 \text{ nm}$) of C6 in CB. Identical spectra were obtained for a solution of C11. These spectra are characteristic of the carbazole monomer.⁶⁰ The fluorescence quantum yields of C6 and C11 in CB amount to, respectively, 0.41 ± 0.04 and 0.45 ± 0.04 . The fluorescence quantum

yields of C6 and C11 covered QDs were estimated to 0.63 ± 0.06 and 0.62 ± 0.06 , respectively (Supplementary material). Here, one should note that the similar fluorescence decay of LCA, C6 and C11 coated QDs (Figure S1)⁵⁵ suggests that no photo-induced hole transfer occurs between the VB of the QD and the HOMO of the carbazole ligands. Compared to the solutions of C6 and C11, the PL spectrum

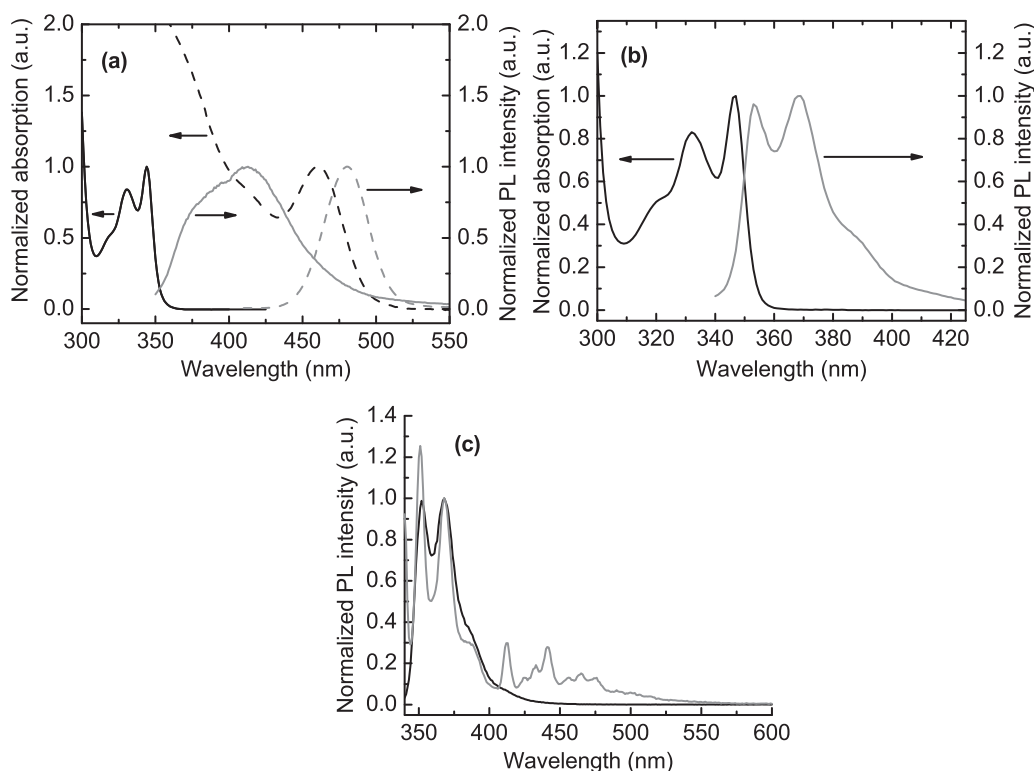


FIG. 3. (a) Optical absorption (black) and PL (gray) spectra of a PVK film (solid) and LCA capped CdSe/ZnS QDs dissolved in CB (dashed). The PL spectra were collected using the excitation of 330 and 400 nm, respectively, for PVK and the QD sample. (b) Optical absorption (black) and PL spectra (gray) of a solution of C11 in CB. In (a) and (b), the absorption spectra are normalized to one at the first maximum of the PVK absorption and the first maximum of the QD absorption. The PL spectra are normalized at the maximum. (c) PL spectra of C11 in methyl-THF solution at room temperature (black) and at 77 K (grey). The emission spectra are normalized at the maximum of the carbazole emission.

of the neat PVK film in Fig. 3(a) shows additional maxima at longer wavelengths due to different types of inter- and intra-chain excimers^{43,52} and has a significantly lower fluorescence quantum yield of 0.16 ± 0.03 . Fig. 3(c) shows the PL spectrum ($\lambda_{\text{exc}} = 330$ nm) of a solution of C11 in methyl-THF measured at 77 K and at room temperature (RT). The additional peaks at longer wavelength (0-0 transition at 410 nm or 3.01 eV) observed at 77 K are attributed to phosphorescence of the carbazole moieties which can only be observed at low temperature. When comparing the absorption spectrum of the QDs in Fig. 3(a) with the phosphorescence spectrum of the carbazole moiety in Fig. 3(c) (which is expected to be unaltered in the film) it is clear that also triplet-triplet transfer from carbazole to the QDs should be possible.

After ligand exchange by the carbazole ligands, the absorption and PL spectra ($\lambda_{\text{exc}} = 330$ nm) of the QDs in CB show bands of both the carbazole monomer and the CdSe core, as illustrated in Fig. 4. As in Fig. 4(a), the absorption spectra are normalized to one at the maximum of the absorption band of the QDs, the approximate amount of C6 and C11 per dot after the ligand exchange can be compared considering the ratio of the absorption of the QDs and that of the carbazole ligands. This approach suggests that the number of C6 ligands per QD is slightly higher than that of C11 ligands per QD, which is in line with the information obtained from the ¹H NMR spectra. When the samples are excited at 330 nm where light absorption is nearly exclusive by the carbazole moiety, the QD core emission of the C6 capped QD sample is however significantly more intense than that of the C11 capped QD sample. For both the C6 and C11 capped QDs, it was also observed that the intensity of the QD emission upon excitation at 330 nm is significantly higher than when a solution with the same concentration of LCA capped QDs is excited at 330 nm (where only the QDs absorb at 330 nm). This suggests that the QD core emission is enhanced significantly by energy transfer from the carbazole group of the ligands. In addition, Fig. 4(b) suggests that the energy transfer is more efficient in the case of the shorter ligand (C6). This is no surprise as energy transfer (whether singlet or triplet) shows a strong distance dependence and one would expect that the average distance between the carbazole antenna and the CdSe core is smaller in the C6 capped QDs than in the C11 capped QDs.

In a next step, the absorption and stationary PL spectra of PVK films doped with QDs capped with LCA, C6, and C11 will be compared. Table I gives the composition of PVK films doped with QDs expressed in wt. % of LCA capped QDs, vol. % of CdSe cores, and the fraction of 330 nm radiation absorbed by the QD cores at each concentration. For LCA capped QDs, the concentrations in wt. % of QDs and vol. % of CdSe cores were calculated from information provided in the product's datasheet (the concentration in mg/ml and total molecular weight of the QDs with LCA coating) while the core diameter was estimated from the absorption maximum of the QDs.

The fraction of the radiation absorbed by CdSe was calculated from the extinction coefficients of PVK and of the QDs at 330 nm. For the samples where LCA ligands were exchanged by C6 or C11, the concentration of QDs in wt. % was estimated from the absorption at 460 nm in CB solution. Here, we did not take into account that the molecular weight of a C6 or C11 capped QD is slightly different from that of an LCA capped QD due to a different molecular weight of the ligands and a different number of ligands per QD. In the case of PVK doped with QDs with C6 and C11 capping, the percentage of the radiation absorbed by CdSe will be even lower for the same concentration, since also the carbazole ligands strongly absorb 330 nm radiation. However, our aim of presenting these values is only to estimate whether the QD emission could be due to direct excitation of the QDs.

Optical absorption and PL spectra of pristine PVK and doped PVK films with different concentrations of LCA capped QDs are presented in Figs. 5(a) and 5(b), respectively. Due to the significantly higher extinction coefficient of PVK (~20 times higher for a monomer than that of a single CdSe pair in a QD), the absorption spectra of the doped PVK films below 350 nm at all concentrations are dominated by the absorption of PVK. The long wavelength tail of the absorption spectrum which becomes more important upon increasing the concentration of the QDs is mainly due to light scattering by the QDs and suggests aggregation of the QDs. At a concentration of QDs up to 30 wt. %, the PL spectra show that energy transfer to the QD cores is apparently still inefficient. Only for samples with 20 and 30 wt. % QDs, a weak QD core emission with maximum at 480 nm is found, which was probably to a large extent due to direct absorption by the QD cores at 330 nm.

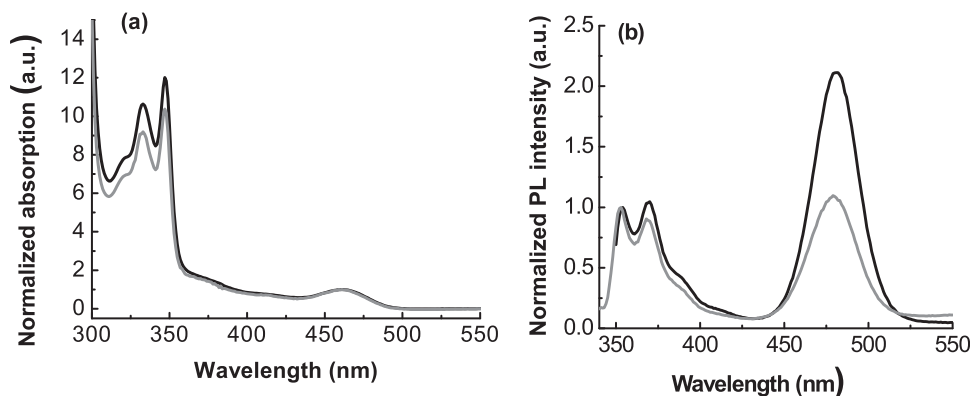


FIG. 4. Optical absorption (a) and PL ($\lambda_{\text{exc}} = 330$ nm) spectra (b) of CdSe/ZnS QDs after the ligand exchange by C6 (black) and C11 (grey) (solution in CB). The absorption spectra were normalized to one at the maximum of the first QD absorption band. The emission spectra are normalized at the first maximum of the carbazole absorption.

TABLE I. The estimated concentrations in vol. % of CdSe corresponding to the doping concentrations in wt. % of LCA capped QDs in doped PVK films and the percentage of the 330 nm radiation absorbed by CdSe at each wt. %.

wt. % QDs (LCA)	vol. % CdSe	% light absorbed by CdSe (330 nm)
5	0.9	0.26
10	1.8	0.55
20	3.6	1.23
30	5.4	2.10

These results were unexpected as assuming a diameter of 2.05 nm for the CdSe core (*cfr supra*) the average distance from a carbazole moiety to a QD is only 2 nm or less at a

loading of 30 wt. %. Under those conditions efficient singlet transfer from carbazoles to the QDs would be expected. This deviation could be due to aggregation of the QDs due to limited miscibility of the LCA ligands and the PVK matrix as already suggested by the light scattering in the absorption spectra.

Therefore, we studied the morphology of the mixed films using transmission microscopy and confocal fluorescence microscopy (Figs. 6(a) and 6(d)). The confocal microscopy images were obtained for an excitation wavelength of 440 nm (only absorbed by QDs) in order to see only emission from the QD cores. These micrographs clearly show the appearance of structures with a size of 2 to 3 μm at a loading of 30 wt. %, indicating aggregation of a large number of

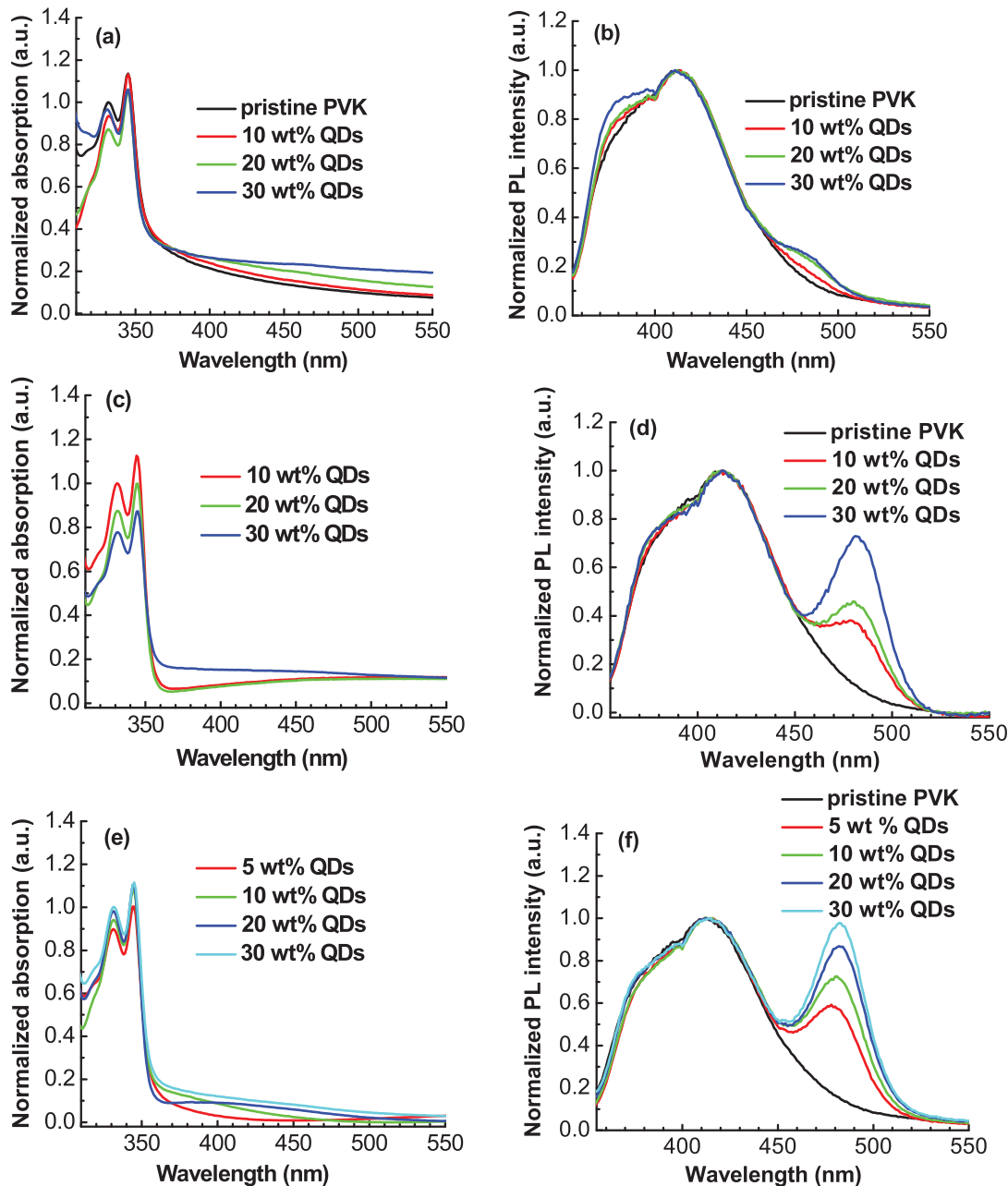


FIG. 5. Optical absorption and PL (normalized to one at the maximum of the carbazole emission) spectra of doped PVK films with QDs capped with LCA ligands ((a) and (b)), C6 ((c) and (d)), and C11 ((e) and (f)). Note that the concentrations in wt. % of QDs after the ligand exchange by C6 and C11 refer to the concentration of the starting QDs with LCA ligand.

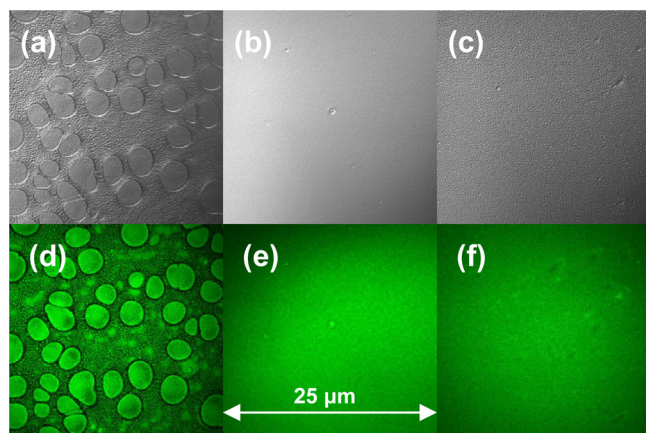


FIG. 6. Transmission (a–c) and confocal fluorescence (d–f) microscopy images of doped PVK films with LCA capped QDs ((a) and (d)), C6 capped QDs ((b) and (e)), and C11 capped QDs ((c) and (f)) at 30 wt. % of QDs. The confocal fluorescence microscopy images were obtained with excitation at 440 nm, which is only absorbed by QD cores. The image size corresponds to $\sim 25 \times 25 \mu\text{m}$.

QDs. Therefore, we developed the C6 and C11 ligands hoping to get better miscibility with the PVK matrix. Figs. 6(b) and 6(e) and 6(c) and 6(f) show that at a loading of 30 wt. % of, respectively, C6 and C11 capped QDs, the film structure is homogeneous at the resolution of transmission ($1 \mu\text{m}$) and confocal fluorescence microscopy (200 to 300 nm).

Figs. 5(c)–5(f) illustrate optical absorption and PL spectra of the doped PVK films with the QDs after the ligand exchange to C6 and C11. The absorption spectra show in agreement with the micrographs a reduction of the light scattering indicating that at the same loading there are less or smaller aggregated particles. Furthermore at all doping concentrations, we observed upon excitation of the carbazole (of the film and the capping layer) a strong increase of the QD emission. Considering the small fraction of light absorbed by the QDs and the fluorescence QYs of the PVK film (0.16 ± 0.03) and of the QDs (with C11 ligands) in a PVK film (0.30 ± 0.06 , see Supplementary material), this suggests the occurrence of energy transfer either in the singlet or on the triplet manifold. In contrast to the PL spectra of the C6 and C11 capped QDs in solution (Fig. 4(b)), the doped PVK films with C11 capped QDs suggest a more efficient energy transfer to QD cores than that with C6 capped QDs. Here, one should note the similarity between the

fluorescence decay of C11 capped QDs in PVK and polystyrene (Figure S2)⁵⁵ suggests that no photo-induced hole transfer occurs between the VB of the QD and the HOMO of PVK.

C. Time-resolved PL experiments

As both singlet and triplet energy transfers from carbazole to the QDs are in principle possible according to overlap of the fluorescence and phosphorescence spectra of carbazoles and the absorption spectrum of the QDs, it is important to determine the efficiency of at least one of those processes in an independent way. The singlet energy transfer efficiency can be estimated from the fluorescence decay of the donor (carbazole) in the absence and presence of acceptors (QDs). Fig. 7 illustrates the fluorescence decays of free and bound C6 (a) and C11 (b) in CB solution. The excitation wavelength and the recorded emission wavelength were 330 and 354 nm, respectively. The fluorescence decay of the carbazole emission of C6 and C11 capped QDs, recorded by single photon timing, can be analyzed as a sum of two exponentials (Eq. (1)) yielding the decay parameters (decay times (τ_i) and amplitudes (A_i)) shown in Table II

$$I(t) = A_1 \exp\left(\frac{-t}{\tau_1}\right) + A_2 \exp\left(\frac{-t}{\tau_2}\right). \quad (1)$$

The excitation occurred at 330 nm and the emission was recorded at 354 nm. The efficiencies of fluorescence resonance energy transfer (FRET) (Φ_{ET}) from carbazole moieties to the QD cores were estimated according to Eq. (3).

For free C6 and C11, the major component has a fluorescence decay time of $7.27 \pm 0.02 \text{ ns}$ which corresponds to literature values of *N*-ethylcarbazole or *N*-isopropylcarbazole.⁶⁰ The fast decay component, which contributes only 3%–4% to the stationary fluorescence, is probably due to an impurity. For C6 and C11 bound to the QDs, a component with an amplitude of 68% (C6) to 77% (C11) and a decay time of 7.3 to 7.4 ns is accompanied by a component with a decay time from 2.4 ns (C6) to 2.7 ns (C11) and an amplitude of 32% (C6) and 23% (C11). As the NMR experiments indicate that no unbound C6 and C11 is present in the solutions, all emission is due to C6 and C11 molecules bound to QDs. Therefore, this non-single-exponential decay suggests a

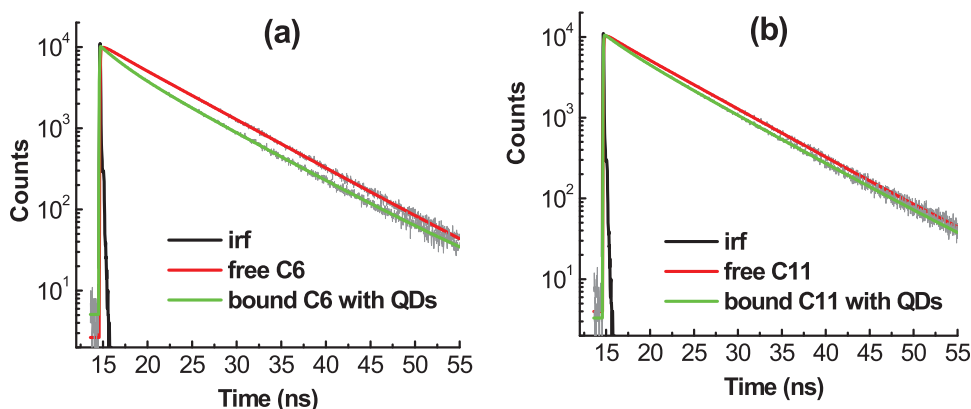


FIG. 7. Fluorescence decays of free and bound ligands in CB solution; (a) gives the decays obtained for C6 while (b) gives those obtained for C11. The λ_{exc} and the λ_{em} are 330 and 354 nm, respectively. The black line in both pictures represents instrument response function (IRF). The gray lines are the measured decays while the red and green lines are fits according to Eq. (1).

TABLE II. PL decay times and amplitudes of the fluorescence decays of free and bound ligands, C6 and C11 analyzed as bi-exponential decay.

Sample	A ₁ (%)	τ ₁ (ns)	A ₂ (%)	τ ₂ (ns)	Φ _{ET} (%)
Free C6	3	2.65	97	7.29	...
Bound C6	32	2.43	68	7.31	19.6
Free C11	4	2.65	96	7.25	...
Bound C11	23	2.74	77	7.37	10.8

distribution of conformations of the alkyl chains and hence of distances between the donor (carbazole) and the acceptor (QD). Although the decay could be fitted to a sum of two exponentials, it is probably more complex. As both decay times did not differ too much, it makes sense to define an amplitude-weighted average fluorescence decay time given by

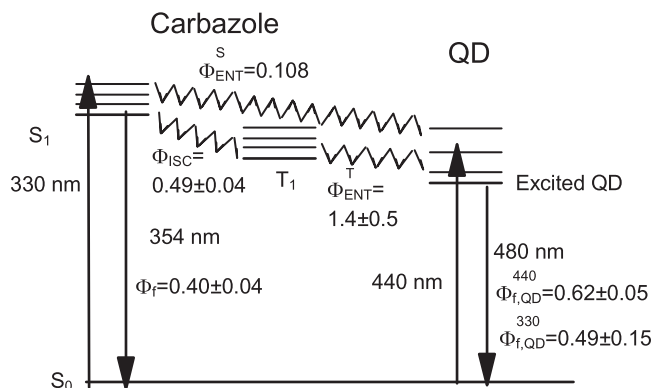
$$\langle \tau \rangle = A_1 \tau_1 + A_2 \tau_2. \quad (2)$$

In this way, the efficiency of the FRET can then be estimated by following expression:

$$\Phi_{ET} = 1 - \frac{\langle \tau_{DA} \rangle}{\langle \tau_D \rangle}, \quad (3)$$

where Φ_{ET} is the energy transfer efficiency, $\langle \tau_D \rangle$ and $\langle \tau_{DA} \rangle$ are the amplitude-weighted fluorescence decay time of the donor (carbazole) in the absence and presence of the acceptor (QDs), respectively.⁶¹ Equation (3) assumes that the rate constants for fluorescence and radiationless decay are the same in free and bound C6 and C11.

By applying Eqs. (2) and (3), FRET efficiencies of 19.6% and 10.8% were obtained for the case of C6 and C11 bound to QDs, respectively. According to the steady-state PL spectra in Fig. 4(b), more efficient energy transfer from carbazoles to QD cores is found for the shorter ligand. The relatively small efficiency for the energy transfer is due on one hand to the large distance between the carbazoles and the CdSe core (which is shielded by the ZnS shell) and on the other hand to the low transition dipole per CdSe unit in the QDs. A Jablonski diagram presenting the photochemical processes taking place in C11 molecules upon $\lambda_{exc} = 330$ nm and $\lambda_{em} = 354$ nm and 480 nm is illustrated in Scheme 1. The ISC yields and fluorescence yields of bound C11 were estimated based on the values obtained from the efficiency for FRET, the fluorescent QYs of the free ligands at $\lambda_{exc} = 330$ nm and the assumption that the S_1 state of the free ligand does not undergo internal conversion.⁶² In spite of the relatively inefficient singlet transfer from carbazole to the QDs, intense emission of the QDs is observed upon excitation of carbazole, suggesting an overall efficient energy transfer. If, e.g., for the C11 capped QDs the excitation occurred only by singlet transfer, their fluorescence quantum yield would amount to $(0.62 \pm 0.06) \cdot 0.108 = 0.068 \pm 0.007$ while on the other hand the fluorescence quantum yield of the carbazole would be $(0.45 \pm 0.05) \cdot (1 - 0.108) = 0.40 \pm 0.04$. However, Figure 4(b) shows that the intensity of the QD emission is nearly twice as large as that of the carbazole moiety



SCHEME 1. Jablonski diagram of the CdSe/ZnS QD with a C11 ligand in CB solution.

instead of eight times smaller. This suggests the occurrence of triplet-triplet transfer between carbazoles and the QDs and efficient emission from QDs originally excited to their triplet excited state by triplet-triplet energy transfer. For the C11 ligands, the efficiency for triplet transfer was estimated to $140 \pm 50\%$ (details of calculation see Supplementary material).⁵⁵ Due to higher energy level of the carbazole triplet state (3.01 eV) compared to the band gap of the QDs (2.65 eV) and the high ISC quantum yield in carbazoles (0.59 ± 0.06 and 0.55 ± 0.06 for C6 and C11, respectively), efficient triplet state transfer is possible.

The estimated values of ISC and fluorescence yields at $\lambda_{em} = 354$ nm were calculated based on the energy transfer efficiencies and fluorescent QYs of free carbazole ligand in CB. In these calculations, it was assumed that in analogy to carbazole⁶² the quantum yield of internal conversion of C11 amounts to zero. The fluorescence quantum yield of the QD emission amounted to 0.62 ± 0.06 and 0.49 ± 0.05 upon excitation at 440 and 330 nm, respectively (see Supplementary material for details). The efficiency for triplet energy transfer was calculated as indicated in the Supplementary material.

In a next step, the efficiency of energy transfer to the QDs involving the singlet state of carbazoles in the doped PVK films was investigated by recording the fluorescence decay of poly-vinylcarbazole in the absence and presence of QDs capped with carbazole ligands. One should note that the polymer matrix itself has a complex photophysics. Besides the emission from carbazole monomer, emission from partial and full overlap excimers of carbazole is also observed. Furthermore, energy transfer from the monomer to both types of excimers can occur.⁴³ The PL spectrum (Fig. 3) shows that most of the emission is due to the full overlap excimer (maximum around 415 nm or 2.99 eV) while a smaller part of the emission can be attributed to the partial overlap excimer (shoulder at 390 nm). When doped with carbazole capped QDs the terminal carbazole moieties of the ligands can also be involved in the formation of the excimers with carbazole moieties pending from the PVK chain. In the PVK film, the PL spectra suggest that the excitation mainly gets trapped in the full overlap excimer sites. The extent of the energy transfer from the latter sites to the QDs was investigated by recording the fluorescence decay at 430 nm for a neat PVK

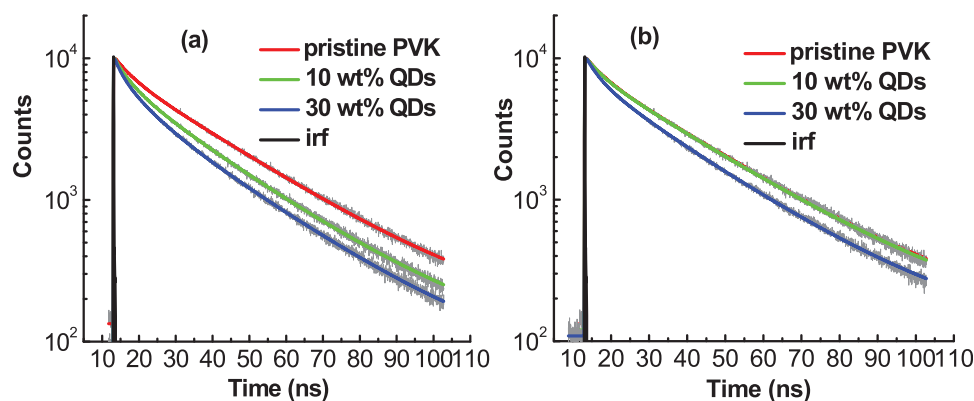


FIG. 8. Fluorescence decays of neat PVK and doped PVK films with C6 (a) and C11 (b) capped QDs recorded at $\lambda_{em}=430$ nm. Excitation occurred at 330 nm. The gray lines are the measured decays while the red, blue, and green lines are fits according to Eq. (1).

film and doped PVK films with 10 wt. % and 30 wt. % of C6 and C11 capped QDs (Fig. 8). The fluorescence decays could be analyzed as a sum of two exponentials of which the amplitudes and decay times are presented in Table III.

The emission was recorded at 430 nm and excitation occurred at 330 nm. The efficiencies of FRET (Φ_{ET}) to the QDs were estimated according to Eq. (3) and decay times are presented in Table III. By applying Eqs. (2) and (3), FRET efficiencies of 18% and 28.4% were obtained for PVK films doped with 10 wt. % and 30 wt. % QDs (C6), while 0% and 16% for the films doped with 10 wt. % and 30 wt. % QDs (C11). The absence of singlet transfer in PVK films doped with 10 wt. % C11 capped QDs corresponds also in qualitative way (Figure 8(b)) with the coincidence of the fluorescence decays of pristine PVK and PVK with 10 wt. % C11 capped QDs. The inefficient singlet energy transfer can be attributed to the fact that only direct (i.e., not mediated by exciton hopping between carbazole moieties) energy transfer between carbazole and the QDs is possible. The inefficient exciton diffusion in PVK can be attributed to the strong red shift of the excimer emission compared to the absorption of carbazole, which makes exciton hopping between excimer sites highly improbable. However, the steady state spectra (Fig. 5(f)) suggest that already at 5 and 10 wt. % doping quite efficient energy transfer already occurs. At 10% doping the triplet energy transfer had, e.g., an efficiency of $17 \pm 9\%$ (for details of calculation, see Supplementary material).⁵⁵ This suggests in analogy with the results obtained for the QDs in solutions that energy transfer from the triplet state of carbazole to the QDs is an important process in PVK doped with C11 capped QDs.

TABLE III. PL decay times and amplitudes of the fluorescence decays of pristine PVK films and doped PVK films with 10 wt. % and 30 wt. % of C6 and C11 capped QDs analyzed as a bi-exponential decay.

Sample	A ₁ (%)	τ_1 (ns)	A ₂ (%)	τ_2 (ns)	Φ_{ET} (%)
Pristine PVK film	22.5	4.5	77.5	25.9	...
10% QDs (C6)	34.5	4.7	65.5	23.9	18.0
30% QDs (C6)	42.5	4.5	57.5	22.9	28.4
10% QDs (C11)	22.4	4.6	77.6	25.9	0
30% QDs (C11)	33.3	4.6	66.7	24.3	16.0

IV. CONCLUSION

Ligand exchange where the LCA ligands are replaced with ligands that are miscible with PVK due to the presence of a terminal carbazole moiety enhances the sensitized QD emission of colloidal CdSe/ZnS QDs in a PVK matrix. Quantitative NMR experiments and stationary UV-Vis absorption showed that a major part of the LCA ligands were exchanged by C6 and C11. Both approaches suggested that ligand exchange by C6 was more efficient than that by C11. Combination of stationary and time-resolved fluorescence experiments suggested that the excitation transfer from the ligands to the QDs was more efficient for a solution of C6 capped QDs than for a solution of C11 capped QDs, which can be attributed to a smaller average distance of the carbazole moiety to the CdSe core in QDs capped with C6. Contrary to the stationary fluorescence spectra, the fluorescence decays of the carbazole chromophore suggested only a modest efficiency for the energy transfer from the singlet excited state of carbazole to the QDs. This suggests that a major part of the energy transfer occurs in the triplet manifold which is populated with a quantum yield of ISC amounting to 0.59 ± 0.06 and 0.55 ± 0.06 for the C6 and C11 capped QDs, respectively. As the triplet energy transfer probably occurs by Dexter transfer which has only a limited range, it is no surprise that this process is more efficient for C6 than for C11.

The inefficient energy transfer between the PVK matrix and LCA capped QDs was attributed to clustering of the QDs, which was also shown in transmission and confocal fluorescence micrographs. As this efficiency is improved significantly after the ligand exchange, where also the optical transmission and confocal microscopy images suggest a homogeneous mixing at the resolution of the micrographs, this phenomenon is probably due to a better miscibility of C6 and C11 capped QDs. In analogy with the experiments on solutions of C6 and C11 capped QDs, the combination of efficient overall energy transfer with the relatively inefficient quenching of the carbazole singlet by the QDs suggests that the emitting state of the QDs is mainly populated by triplet transfer from the carbazoles. Generally triplet energy transfer is expected to happen by Dexter transfer (electron exchange), which requires a very short distance between donor and acceptor. As in the PVK films only a limited fraction of carbazoles is in direct contact with the QDs the energy transfer

must be preceded by triplet energy hopping between the carbazoles until a triplet state of a carbazole ligand is populated. As for the triplet state exciton interaction is several orders of magnitude smaller than for the singlet state the partially and fully overlapped carbazole excimers are expected to figure as less efficient traps for the triplet allowing efficient triplet hopping. In contrast to the QD solutions, the doped PVK films with C11 capped QDs show more efficient overall energy transfer but less efficient singlet transfer than those of C6 capped QDs which suggests a better mixing for the latter QDs. Finally, the results also show that at room temperature the excited state of the QDs populated after triplet transfer is either a good emitter or converted efficiently in an emitting state of the QDs. It cannot be excluded that in OLEDs the relative intensity of the QD emission (*vs.* the carbazole emission) is even larger as in principle the QDs can also act as recombination centers where the exciton formation occurs. The decrease of the average fluorescence decay time and quantum yield of the QDs upon incorporation in a polymer matrix (see Supplementary material) suggests that it remains necessary to develop ligands that bind better to the QD or cover the QD more completely in order to have an efficient conversion of the triplet excitons formed in an OLED setting into photons.

ACKNOWLEDGMENTS

The authors thank the Research Fund of the K.U.Leuven for financial support through GOA2006/2 and ZWAP 4/07 and the Belgium Science Policy through IAP 6/27 and 7/05. The authors thank the EU through the Marie Curie network “Herodot” (Grant 214954) for a fellowship to A.K. and A.H. The authors thank IMEC for a fellowship to Y.F. and the “Instituut voor de aanmoediging van innovatie door Wetenschap en Technologie in Vlaanderen” (IWT) is acknowledged for a fellowship to L.P. The authors are indebted to the FWO for a doctoral fellowship to C.D. and a research grant to Z.H. (Project G.0479.10).

- ¹K. Müllen and U. Scherf, *Organic Light-Emitting Devices* (Wiley-VCH, Weinheim, 2006).
- ²P. Chen, Q. Xue, W. Xie, Y. Duan, G. Xie, Y. Zhao, J. Hou, S. Liu, L. Zhang, and B. Li, *Appl. Phys. Lett.* **93**, 153508 (2008).
- ³T. Peng, G. Li, Y. Liu, Y. Wu, K. Ye, D. Yao, Y. Yuan, Z. Hou, and Y. Wang, *Org. Electron.* **12**, 1068 (2011).
- ⁴M. A. Baldo, S. Lamansky, P. E. Burrows, M. E. Thompson, and S. R. Forrest, *Appl. Phys. Lett.* **75**, 4 (1999).
- ⁵D. F. O'Brien, M. A. Baldo, M. E. Thompson, and S. R. Forrest, *Appl. Phys. Lett.* **74**, 442 (1999).
- ⁶J. P. Duan, P. P. Sun, and C. H. Cheng, *Adv. Mater.* **15**, 224 (2003).
- ⁷Z. Hong, C. Liang, R. Li, W. Li, D. Zhao, D. Fan, D. Wang, B. Chu, F. Zhang, L. S. Hong, and S. T. Lee, *Adv. Mater.* **13**, 1241 (2001).
- ⁸Q. Xin, W. L. Li, W. M. Su, T. L. Li, Z. S. Su, B. Chu, and B. Li, *J. Appl. Phys.* **101**, 044512 (2007).
- ⁹C. Adachi, M. A. Baldo, M. E. Thompson, and S. R. Forrest, *J. Appl. Phys.* **90**, 5048 (2001).
- ¹⁰I. Tanaka, Y. Tabata, and S. Tokito, *Chem. Phys. Lett.* **400**, 86 (2004).
- ¹¹H. Yersin, *Highly Efficient OLEDs With Phosphorescent Materials* (Wiley-VCH, Weinheim, 2008).
- ¹²H. H. Liao, H. F. Meng, S. F. Horng, W. S. Lee, J. M. Yang, C. C. Liu, J. T. Shy, F. C. Chen, and C. S. Hsu, *Phys. Rev. B* **74**, 245211 (2006).
- ¹³J. Kido and Y. Okamoto, *Chem. Rev.* **102**, 2357 (2002).

- ¹⁴D. Tanaka, Y. Agata, T. Takeda, S. Watanabe, and J. Kido, *Jpn. J. Appl. Phys., Part 1* **46**, 117 (2007).
- ¹⁵H. Sasabe, E. Gonmori, T. Chiba, Y. J. Li, D. Tanaka, S. J. Su, T. Takeda, Y. J. Pu, K. I. Nakayama, and J. Kido, *Chem. Mater.* **20**, 5951 (2008).
- ¹⁶C. M. Donega, S. G. Hickey, S. F. Wuister, D. Vanmaekelbergh, and A. Meijerink, *J. Phys. Chem. B* **107**, 489 (2003).
- ¹⁷Y. Araki, K. Ohkuno, T. Furukawa, and J. Saraie, *J. Cryst. Growth* **301**, 809 (2007).
- ¹⁸J. M. Caruge, J. E. Halpert, V. Wood, V. Bulović, and M. G. Bawendi, *Nature Photon.* **2**, 247 (2008).
- ¹⁹A. Gopal, K. Hoshino, S. Kim, and X. Zhang, *Nanotechnology* **20**, 235201 (2009).
- ²⁰B. O. Dabbousi, J. Rodriguez-Viejo, F. V. Mikulec, J. R. Heine, H. Mattoussi, R. Ober, K. F. Jensen, and M. G. Bawendi, *J. Phys. Chem. B* **101**, 9463 (1997).
- ²¹X. Peng, M. C. Schlamp, A. V. Kadavanich, and A. P. Alivisatos, *J. Am. Chem. Soc.* **119**, 7019 (1997).
- ²²A. L. Rogach, N. Gaponik, J. M. Lupton, C. Bertoni, D. E. Gallardo, S. Dunn, N. Li Pira, M. Paderi, P. Repetto, S. G. Romanov, C. O'Dwyer, C. M. Sotomayor Torres, and A. Eychmüller, *Angew. Chem., Int. Ed.* **47**, 6538 (2008).
- ²³L. Xu, K. Chen, H. M. El-Khair, M. Li, and X. Huang, *Appl. Surf. Sci.* **172**, 84 (2001).
- ²⁴G. Schmid, *Nanoparticles: From Theory to Application* (Wiley-VCH, Weinheim, 2004).
- ²⁵P. Chin, R. Hikmet, and R. Janssen, *J. Appl. Phys.* **104**, 013108 (2008).
- ²⁶Z. Tan, F. Zhang, T. Zhu, Z. Ting, J. Xu, A. Y. Wang, J. D. Dixon, L. Li, Q. Zhang, S. E. Mohny, and J. Ruzyllo, *Nano Lett.* **7**, 3803 (2007).
- ²⁷P. O. Anikeeva, C. F. Madigan, J. E. Halpert, M. G. Bawendi and V. Bulovic, *Phys. Rev. B* **78**, 085434 (2008).
- ²⁸D. I. Son, D. H. Park, W. K. Choi, and T. W. Kim, *Nanotechnology* **20**, 275205 (2009).
- ²⁹W. K. Bae, J. Kwak, J. W. Park, K. Char, C. Lee, and S. Lee, *Adv. Mater.* **21**, 1690 (2009).
- ³⁰P. Jing, X. Yuan, W. Ji, M. Ikezawa, Y. A. Wang, X. Liu, L. Zhang, J. Zhao, and Y. Masumoto, *J. Phys. Chem. C* **114**, 19256 (2010).
- ³¹K. Matras-Postolek and D. Bogdal, *Adv. Polym. Sci.* **230**, 221 (2010).
- ³²J. Kwak, W. K. Bae, M. Zorn, H. Woo, H. Yoon, J. Lim, S. W. Kang, S. Weber, H. J. Butt, R. Zentel, S. Lee, K. Char, and C. Lee, *Adv. Mater.* **21**, 5022 (2009).
- ³³B. H. Kang, J. S. Seo, S. Jeong, J. Lee, C. S. Han, D. E. Kim, K. J. Kim, S. H. Yeom, D. H. Kwon, H. R. Kim, and S. W. Kang, *Opt. Express* **18**, 18303 (2010).
- ³⁴C. Borriello, S. Masala, V. Bizarro, G. Nenna, M. Re, E. Pesce, C. Minarini, and T. Di Luccio, *J. Appl. Polym. Sci.* **122**, 3624 (2011).
- ³⁵Y. Q. Li, A. Rizzo, M. Mazzeo, L. Carbone, L. Manna, R. Cingolani, and G. Gigli, *J. Appl. Phys.* **97**, 113501 (2005).
- ³⁶H. Mattoussi, L. H. Radzilowski, B. O. Dabbousi, E. L. Thomas, M. G. Bawendi, and M. F. Rubner, *J. Appl. Phys.* **83**, 7965 (1998).
- ³⁷A. Rizzo, Y. Li, S. Kudara, F. Della Stella, M. Zanella, W. J. Parak, R. Cingolani, L. Manna, and G. Gigli, *Appl. Phys. Lett.* **90**, 051106 (2007).
- ³⁸I. Gur, N. A. Fromer, M. L. Geier, and A. P. Alivisatos, *Science* **310**, 462 (2005).
- ³⁹V. I. Klimov, *Los Alamos Sci.* **28**, 214 (2003).
- ⁴⁰R. C. Powell and Q. Kim, *J. Lumin.* **6**, 351 (1973).
- ⁴¹A. Itaya, H. Sakai, and H. Masuhara, *Chem. Phys. Lett.* **146**, 570 (1988).
- ⁴²C. W. Ko and H. C. Lin, *Thin Solid Films* **363**, 81 (2000).
- ⁴³A. Rivaton, B. Mailhot, G. Derderian, P. O. Bussiere, and J. L. Gardette, *Macromolecules* **36**, 5815 (2003).
- ⁴⁴M. B. Khalifa, D. Vaufrey, A. Bouazizi, J. Tardy, and H. Maaref, *Mater. Sci. Eng., C* **21**, 277 (2002).
- ⁴⁵P. Wu, L. G. Yang, H. Ye, X. Liu, L. C. Zeng, X. Gua, S. L. Lu, and M. J. Yang, *J. Mater. Sci.* **39**, 5837 (2004).
- ⁴⁶Y. Xuan, D. Pan, N. Zhao, X. Ji, and D. Ma, *Nanotechnology* **17**, 4966 (2006).
- ⁴⁷S. Ambrozovich, M. van der Auweraer, D. Dirin, M. Parshin, R. Vasil'ev, and A. Vitukhnovsky, *J. Russ. Laser Res.* **29**, 526 (2008).
- ⁴⁸K. S. Lee, D. U. Lee, D. C. Choo, T. W. Kim, E. D. Ryu, S. W. Kim, and J. S. Lim, *J. Mater. Sci.* **46**, 1239 (2011).
- ⁴⁹F. Li, T. Guo, and T. Kim, *Appl. Phys. Lett.* **97**, 062104 (2010).
- ⁵⁰J. Pina, J. Seixas de Melo, H. D. Burrows, A. P. Monkman, and S. Navaratnam, *Chem. Phys. Lett.* **400**, 441 (2004).

- ⁵¹A. van Dijken, J. Bastiaansen, N. Kiggen, B. Langeveld, C. Rothe, A. Monkman, I. Bach, P. Stössel, and K. Brunner, *J. Am. Chem. Soc.* **126**, 7718 (2004).
- ⁵²L. Qian, D. Bera, and P. H. Holloway, *Appl. Phys. Lett.* **92**, 053303 (2008).
- ⁵³A. Khetubol, Y. Firdaus, A. Hassinen, S. Van Snick, Z. Hens, W. Dehaen, and M. Van der Auweraer, *Proc. SPIE* **8424**, 84242W-1 (2012).
- ⁵⁴W. W. Yu, L. Qu, W. Guo, and X. Peng, *Chem. Mater.* **15**, 2854 (2003).
- ⁵⁵See supplementary material at <http://dx.doi.org/10.1063/1.4793266> for details of the synthesis and characterization of C6 and C11, the estimation of the fluorescence quantum yields of the quantum dots, and the way the efficiency of triplet energy transfer is calculated.
- ⁵⁶M. Maus, E. Rousseau, M. Cotlet, G. Schweitzer, J. Hofkens, M. Van der Auweraer, F. C. De Schryver, and A. Krueger, *Rev. Sci. Instrum.* **72**, 36 (2001).
- ⁵⁷G. R. Fulmer, A. J. M. Miller, N. H. Sherden, H. E. Gottlieb, A. Nudelman, B. M. Stoltz, J. E. Bercaw, and K. I. Goldberg, *Organometallics* **29**, 2176 (2010).
- ⁵⁸I. Moreels, B. Fritzing, J. C. Martins, and Z. Hens, *J. Am. Chem. Soc.* **130**, 15081 (2008).
- ⁵⁹N. S. Allen, *Photochemistry and Photophysics of Polymer Materials* (John Wiley & Sons, NJ, 2010).
- ⁶⁰I. B. Berlman, *Handbook of Fluorescence Spectra of Aromatic Molecules* (Academic, New York, 1971).
- ⁶¹A. R. Clapp, I. L. Medintz, J. M. Mauro, B. R. Fisher, M. G. Bawendi, and H. Mattoussi, *J. Am. Chem. Soc.* **126**, 301 (2004).
- ⁶²J. A. Barltrop and J. D. Coyle, *Principle of Photochemistry* (Wiley, Chichester, 1978); J. A. Barltrop and J. D. Coyle, *Excited States in Organic Chemistry* (Wiley, London, 1975).